Journal of Alloys and Compounds 506 (2010) 508–512

Contents lists available at ScienceDirect

Journal of Alloys and Compounds

journal homepage: www.elsevier.com/locate/jallcom

Influence of irreversibility on inverse magnetocaloric and magnetoresistance properties of the $(Ni,Cu)_{50}Mn_{36}Sn_{14}$ alloys

I. Dincer*, E. Yüzüak, Y. Elerman

Department of Engineering Physics, Faculty of Engineering, Ankara University, 06100 Besevler, Ankara, Turkey

ARTICLE INFO

Article history:
Received 1 June 2010
Received in revised form 30 June 2010
Accepted 8 July 2010
Available online 15 July 2010

PACS:
81.30.Kf
75.30.Sg
75.47.De

Keywords:
Magnetocaloric effect
Martensitic transition
Magnetoresistance

ABSTRACT

Influence of irreversibility (magnetoplasticity) on inverse magnetocaloric effect and magnetoresistance of the $(Ni,Cu)_{50}Mn_{36}Sn_{14}$ alloys has been investigated by magnetization and resistivity measurements. X-ray powder diffraction patterns indicate that all alloys crystallize in $L2_1$ cubic structure at room temperature. The substitution of Cu for Ni leads to decreasing on the martensitic transition temperature and increasing on the Curie temperature. The magnetic field dependence of magnetization measurements is performed with continuous heating and noncontinuous heating methods to find the influence of irreversibility on magnetocaloric effect. It is observed that the magnetic entropy change depends strongly on magnetization measurement methods. The resistivity measurements show that the $(Ni,Cu)_{50}Mn_{36}Sn_{14}$ alloys have the one-way magnetostructural transition. Magnetoresistance about −46% is observed at magnetostructural transition temperatures.

1. Introduction

Compared with conventional refrigeration, magnetic refrigeration technology has many advantages, such as the absence of harmful gas, less noise, low cost and high efficiency. Magnetic refrigeration is based on the magnetocaloric effect (MCE) which is the isothermal magnetic entropy change or the adiabatic temperature change in magnetic material when it is subjected to a change in external magnetic field. Pecharsky et al. discuss the thermodynamics of the MCE in Ref. [1]. While the MCE is observed in all materials near second-order transition temperature, the giant MCE is observed in the materials undergoing first-order magnetostructural transition [1]. The research on magnetocaloric materials has been mainly focused in rare-earth metals and its alloys, which may show large magnetocaloric properties between low and room temperatures. However, the most important handicaps for using these materials in practical magnetic cooling systems are the expensiveness of raw materials and the magnetic field needed to achieve a high energetic efficiency is usually well above 2 T that cannot be produced using permanent magnet assemblies. Currently, most attention is paid to the pure magnetocaloric properties and materials cost. So, the finding of new and cheaper magnetic substances able to exhibit giant magnetocaloric efficiency in fields below 2 T arises as the main goal of current researches on MCE materials. The giant magnetoresistance (GMR) effect is of much interest because of its potential technological applications in magnetic recording, actuators and sensors. While the GMR effect has been observed in the various multilayers and granular films, the GMR effect has been also observed in some Heusler alloys [2,3].

Since the discovery of martensitic transformation with both phases magnetically ordered in Heusler alloys $Ni_{55}Mn_{20}Ga_{25}$, $Ni_{50}Mn_{50-x}In_x$ $(15 \le x \le 16)$, $Ni_{50}Mn_{50-x}Sn_x$ $(13 \le x \le 15)$ and $Ni_{50}Mn_{50-x}Sb_x$ $(12 \le x \le 13.5)$ [4,5], increasing attention has been paid to study the change in magnetic and electrical properties associated to the first-order reversible magnetostructural transition that originates valuable functional properties such as magnetic superelasticity, large inverse magnetocaloric effect, and large magnetoresistance change [6–10]. According to the studies on these Heusler alloys, by lowering the temperatures, a cubic high-temperature parent austenite phase transforms into an orthorhombic or monoclinic structurally modulated martensite phase. The characteristic temperatures related to the martensitic transformation are the martensite start temperature M_s, the martensite finish temperature M_f, the austenite start temperature A_s and the austenite finish temperature A_f. The results of these studies have emphasized on the potential technological interest of these ferromagnetic shape memory alloys for the development of magnetic actuators, sensors and as magnetic coolant for magnetic refrigeration technology.

The reversibility and irreversibility of the magnetostructural transition are very important for magnetic actuator materials such

* Corresponding author. Tel.: +90 312 203 3452; fax: +90 312 212 7343.
E-mail address: idincer@eng.ankara.edu.tr (I. Dincer).

0925-8388/$ – see front matter © 2010 Elsevier B.V. All rights reserved.
doi:10.1016/j.jallcom.2010.07.066

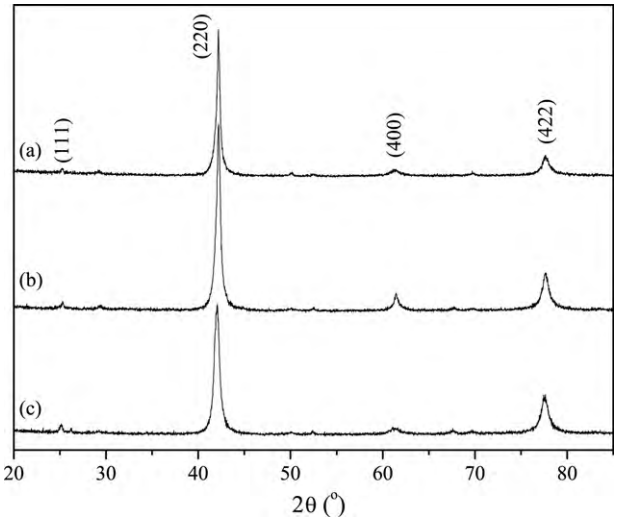

Fig. 1. The X-ray diffraction patterns for $Ni_{46.8}Cu_{2.5}Mn_{36.5}Sn_{14.3}$ (a), $Ni_{45.3}Cu_{4.5}Mn_{35.9}Sn_{14.3}$ (b) and $Ni_{43.1}Cu_{6.5}Mn_{35.9}Sn_{14.5}$ (c).

as magnetic shape memory alloys. The austenite phase induced by the magnetic field is able to transform back to the initial martensite phase when the magnetic field is removed. A complete recovery of the initial martensite state may bring about magnetoelasticity (two-way magnetic shape memory effect), while the irreversible magnetostructural transition would result in magnetoplasticity (one-way magnetic shape memory effect). The reversibility of the magnetostructural transition depends on the alloy system. The results of the study [11] exhibited that the magnetostructural transition in $Ni_{45}Mn_{36.6}In_{13.4}Co_5$ by in situ high-energy synchrotron X-ray diffraction was reversible. According to the studies [12,13], the one-way magnetostructural transition was observed in the $Ni_{50}Mn_{35}Sn_{15}$ and $Ni_{26.5}Mn_{48}Ga_{20}Co_{5.5}$. However, a detailed study about the effects of the irreversibility of the magnetostructural transitions on magnetocaloric effect in the Ni–Mn–Sn alloys is still lacking. We have investigated the influence of the irreversibility of the magnetostructural transition on magnetocaloric and magnetoresistance properties of the (Ni–Cu)–Mn–Sn alloys in this study.

2. Experimental

The $Ni_{50-x}Cu_xMn_{36}Sn_{14}$ (x = 2, 4 and 6) alloys of about 2 g were prepared by arc melting of high-purity elements under argon atmosphere. The alloys were then encapsulated under argon atmosphere in quartz glass and annealed at 1223 K for 2 days to ensure homogeneity. Afterwards, they were quenched in ice water. The composition of the alloys was determined by energy dispersive X-ray (EDX) analysis with using the EVO 40 scanning electron microscope – SEM. The X-ray diffraction experiments with Cu Kα radiation were performed at the room temperature. The magnetization and resistivity measurements were made in a physical properties measurement system PPMS with a magnetic field up to 7 T in the temperature range from 5 to 350 K. Since the $M(T)$ measurements in the different modes give us more information about magnetic properties of the alloys, the temperature dependence of magnetization was measured in zero-field-cooled (ZFC), field-cooled (FC) and field-heated (FH) modes.

3. Results and discussion

The average compositions of the $Ni_{50-x}Cu_xMn_{36}Sn_{14}$ (x = 2, 4 and 6) alloys, calculated from EDX, were found to be $Ni_{46.8}Cu_{2.5}Mn_{36.5}Sn_{14.3}$, $Ni_{45.3}Cu_{4.5}Mn_{35.9}Sn_{14.3}$ and $Ni_{43.1}Cu_{6.5}Mn_{35.9}Sn_{14.5}$. The reported compositions are an average of multiple points on the alloys and no compositional heterogeneity was observed.

XRD experiments confirm that these alloys have an $L2_1$ structure (space group $Fm-3m$) which consists of four interpenetrating fcc sublattices at the room temperature in austenite phase (see Fig. 1).

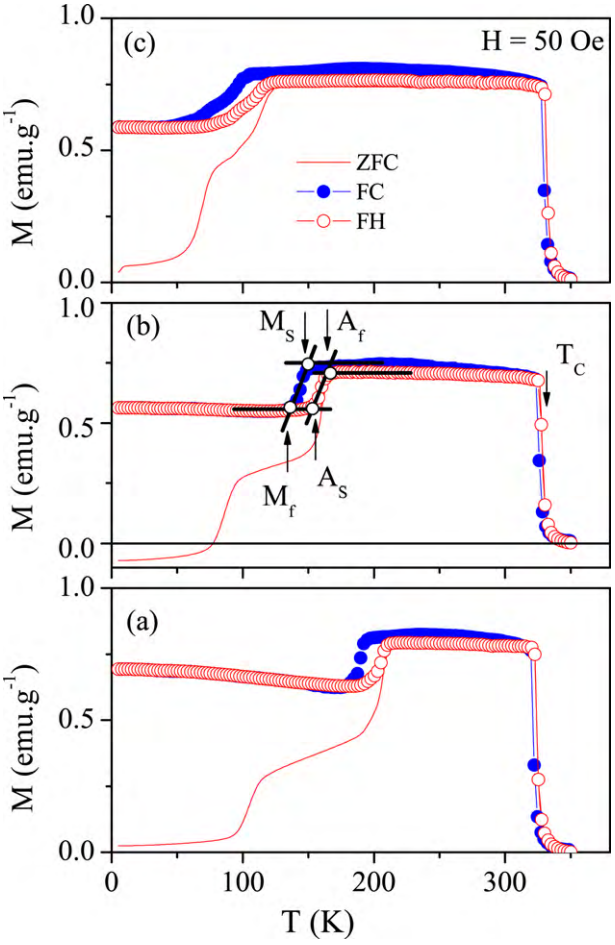

Fig. 2. The ZFC, FC and FH $M(T)$ in 50 Oe of (a) $Ni_{46.8}Cu_{2.5}Mn_{36.5}Sn_{14.3}$, (b) $Ni_{45.3}Cu_{4.5}Mn_{35.9}Sn_{14.3}$ and (c) $Ni_{43.1}Cu_{6.5}Mn_{35.9}Sn_{14.5}$.

The $M(T)$ curves of the $Ni_{46.8}Cu_{2.5}Mn_{36.5}Sn_{14.3}$, $Ni_{45.3}Cu_{4.5}Mn_{35.9}Sn_{14.3}$ and $Ni_{43.1}Cu_{6.5}Mn_{35.9}Sn_{14.5}$ alloys measured from 5 to 350 K in a magnetic field of 50 Oe for ZFC, FC and FH modes are displayed in Fig. 2. All alloys order ferromagnetically in the austenite phase below T_C. With respect to T_C = 317 K of the reference alloy [14,15], T_C increases with increasing Cu concentrations. Below T_C, the temperature dependence of magnetization remains essentially temperature insensitive for all alloys until it begins to drop at M_s. In the vicinity of M_s, the FH curve do not retrace the FC curve but show a narrow hysteresis. When considered together with the results of earlier DSC and XRD studies on similar alloys, the hysteresis can be attributed to a first-order structural transition. Any splitting of the ZFC and FH curves is expected to be associated with pinning due to antiferromagnetic or noncollinear magnetic structures existing with in the ferromagnetic matrix. In these alloys, the coexistence of antiferromagnetic exchange within the ferromagnetic matrix due to excess Mn in the crystal structure is the essential source for nonsaturation. The ZFC curves begin at a low magnetization value due to the essentially random spatial configuration while cooling through T_C down to low temperatures. On heating, the magnetization remains constant until the thermal energy begins to overcome the exchange anisotropy of the frozen state in the 50 Oe measuring magnetic field. At higher temperatures, the ZFC and FH curves merge. The characteristic temperatures of the martensitic transformation are defined as the intersections of extrapolations from linear regions of the data [16]. The valance electron concentrations per atom e/a dependence of M_s in Ni–Mn–Z (Z: Al, Ga, In, Sn, Sb) Heusler alloys is

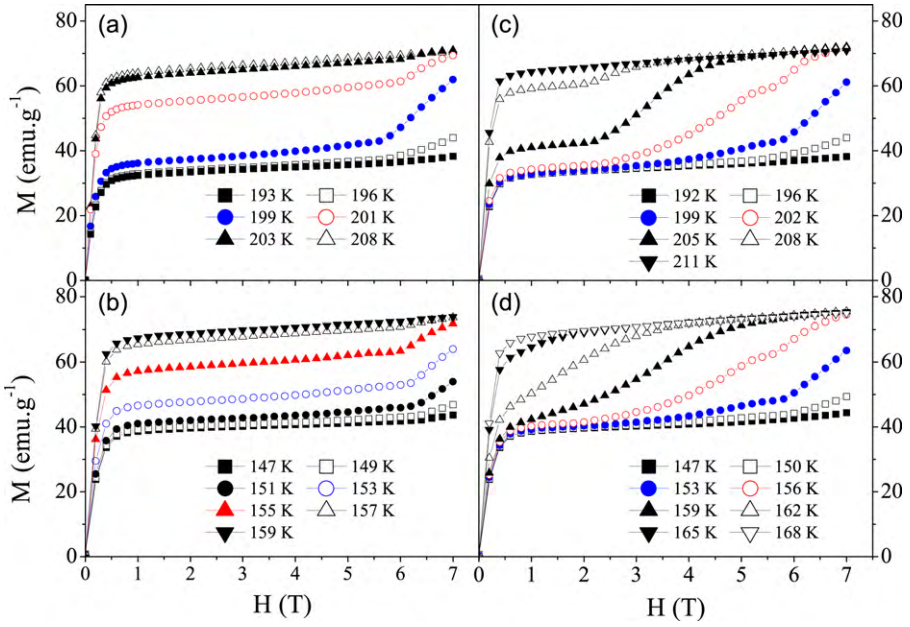

Fig. 3. Isothermal magnetization vs magnetic field of $Ni_{46.8}Cu_{2.5}Mn_{36.5}Sn_{14.3}$ and $Ni_{45.3}Cu_{4.5}Mn_{35.9}Sn_{14.3}$ (a) and (b) for continuous heating, (c) and (d) for noncontinuous heating.

linear, but with different slopes for each Z [17]. As shown in Fig. 2, the characteristic temperatures of the martensitic transformation decrease with increasing Cu concentrations while the valence electron concentrations per atom e/a increase. All of the transition temperatures are shown in Table 1.

Isothermal M–H curves for the $Ni_{46.8}Cu_{2.5}Mn_{36.5}Sn_{14.3}$ and $Ni_{45.3}Cu_{4.5}Mn_{35.9}Sn_{14.3}$ alloys were measured with using two different methods to see the influence of the irreversibility of the magnetostructural transition on the magnetic properties of these alloys. In the first method, after zero-field cooling from 340 K to low temperatures (100 and 50 K for the $Ni_{46.8}Cu_{2.5}Mn_{36.5}Sn_{14.3}$ and $Ni_{45.3}Cu_{4.5}Mn_{35.9}Sn_{14.3}$ alloys, respectively), the temperature went up to the desirable temperature. At this temperature, the magnetic field dependence of magnetization was measured from 0 to 7 T, and subsequently demagnetized from 7 to 0 T. After the magnetization measurement was completed, temperature was increased to next temperature. This measurement method is called as continuous heating. Fig. 3(a) and (b) shows the $M(H)$ curves measured with continuous heating method. In the second method, after the sample was cooled down to lower temperatures (100 and 50 K) from 340 K under zero magnetic field, the temperature was heated to a desirable temperature to measure $M(H)$ curve. At this temperature, the magnetic field dependence of magnetization was measured from 0 to 7 T, and subsequently demagnetized from 7 to 0 T. After the magnetization measurement was completed, the sample was initially zero-field-cooled down to 140 K for $Ni_{46.8}Cu_{2.5}Mn_{36.5}Sn_{14.3}$ and 70 K for $Ni_{45.3}Cu_{4.5}Mn_{35.9}Sn_{14.3}$ to ensure a complete martensite state and then zero magnetic field heated to the next temperature. This sequence is termed as noncontinuous heating method. Fig. 3(c) and (d) shows the $M(H)$ curves measured with noncontinuous heating method.

Table 1
The valence electron concentrations per atom e/a, martensite start and finish temperatures (M_s and M_f) and austenite start and finish temperatures (A_s and A_f) determined from $M(T)$ measurements (M in superscript). The data of the $Ni_{50}Mn_{36}Sn_{14}$ alloy was taken from Refs. [14,15].

Alloy	e/a	M_S^M (K)	M_f^M (K)	A_S^M (K)	A_f^M (K)	T_C (K)
$Ni_{50}Mn_{36}Sn_{14}$	8.080	220	210	240	250	317
$Ni_{46.8}Cu_{2.5}Mn_{36.5}Sn_{14.3}$	8.082	194	182	197	212	321
$Ni_{45.3}Cu_{4.5}Mn_{35.9}Sn_{14.3}$	8.110	148	136	151	167	325
$Ni_{43.1}Cu_{6.5}Mn_{35.9}Sn_{14.5}$	8.118	106	58	76	122	329

Using the data in Fig. 3, the magnetic field induced entropy change ΔS_M is determined by integrating numerically $\Delta S_M = \int_0^H (\partial M/\partial T)_H dH$. ΔS_M for $Ni_{46.8}Cu_{2.5}Mn_{36.5}Sn_{14.3}$ and $Ni_{45.3}Cu_{4.5}Mn_{35.9}Sn_{14.3}$ is shown in Fig. 4(a) and (c) for continuous heating and in Fig. 4(b) and (d) for noncontinuous heating. For the both alloys, $\Delta S_M(T,H)$ is positive (inverse MCE) for continuous heating and noncontinuous heating method, respectively (Fig. 4(a) and (c)). Inverse MCE means that the sample cools when a magnetic field is applied adiabatically. While the peak value of ΔS_M estimated from continuous heating data is 43 and 27 J kg^{-1} K^{-1} for the magnetic field change of 5 T, the peak value of ΔS_M estimated from noncontinuous heating data is 20.9 and 13.1 J kg^{-1} K^{-1} for $Ni_{46.8}Cu_{2.5}Mn_{36.5}Sn_{14.3}$ and $Ni_{45.3}Cu_{4.5}Mn_{35.9}Sn_{14.3}$, respectively. In these alloys, the peak position and value of ΔS_M is closely related to the sample history. At the temperatures between A_s and A_f, the sample is in mixed phase state where coexists martensite and austenite phases. The main phase is martensite phase near A_s and when the magnetic field is increased until to 7 T at this temperature, the main phase of the sample is austenite phase. When the magnetic field reduced to zero, the sample stays in austenite rich phase since the magnetostructural transition in our samples is irreversible. Due to the irreversibility of the transition, the area between two $M(H)$ curves which obtained from continuous heating method is bigger than that of noncontinuous heating method. Therefore, the maximum values of ΔS_M from continuous heating method are bigger than noncontinuous heating method. Caron et al. used loop process that is similar to our noncontinuous heating method for estimating MCE from $M(H)$ curves for some alloys that exhibit magnetostructural transitions with thermal hysteresis [18]. In loop process, after the $M(H)$ measurements the temperature went up to higher temperatures to paramagnetic region instead of the temperature decreasing in our method. Since our samples show inverse MCE unlike the alloys in Ref. [18], we used the noncontinuous heating method. According to the study [18], the peak in the magnetic entropy change is strongly reduced to lower values compared with the values obtained from standard process. The peak value of ΔS_M of our alloys (obtained from noncontinuous heating method) is comparable to the results

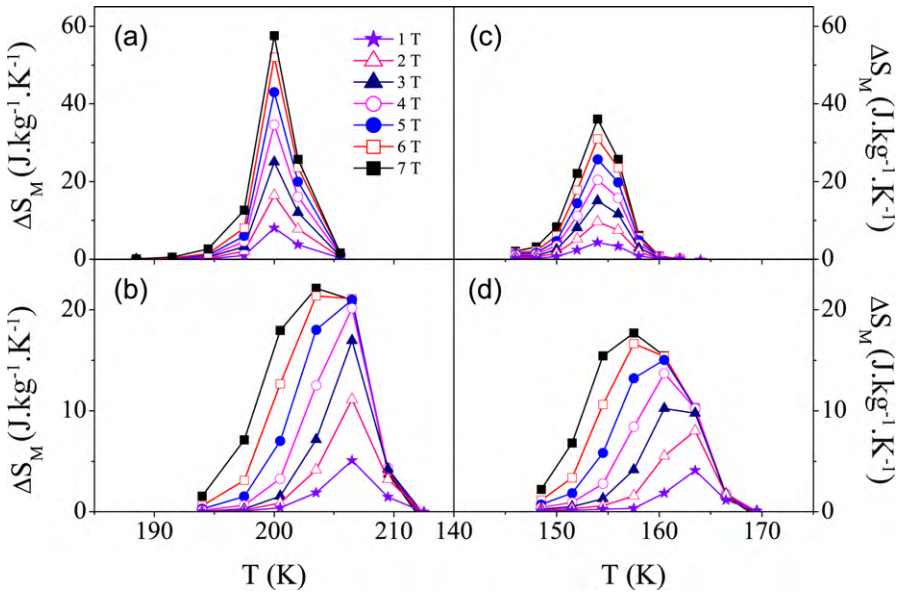

Fig. 4. The temperature dependence of the magnetic entropy change for $Ni_{46.8}Cu_{2.5}Mn_{36.5}Sn_{14.3}$ and $Ni_{45.3}Cu_{4.5}Mn_{35.9}Sn_{14.3}$ (a) and (c) for continuous heating, (b) and (d) for noncontinuous heating.

of $MnFeP_{0.8}Ge_{0.2}$ ($\Delta S_M = -35\,J\,kg^{-1}\,K^{-1}$), $La_{0.8}Ce_{0.2}Fe_{11.4}Si_{1.6}$ ($\Delta S_M = -30\,J\,kg^{-1}\,K^{-1}$), $Mn_{0.99}Cu_{0.01}As$ ($\Delta S_M = -45\,J\,kg^{-1}\,K^{-1}$) and $Gd_5Ge_{2.3}Si_{1.7}$ ($\Delta S_M = -35\,J\,kg^{-1}\,K^{-1}$) alloys (obtained from loop process) for the magnetic field change of 5 T [18].

When characterizing materials exhibiting giant MCE, two magnetic measurement methods are necessarily performed:

(i) Isofield measurements ($M(T)$ curves under different magnetic fields) to determine the critical temperature, thermal hysteresis.
(ii) Isothermal measurements ($M(H)$ curves at the different temperatures) that are used to estimated isothermal entropy change using the Maxwell relations.

Both measurement methods explore the same phenomenon, and therefore should be equivalent. For reversible processes, the equivalence of these two processes is correctly achieved. However, when measuring a material showing magnetostructural transition (with large hysteresis), where a magnetization process is not fully reversible, history-dependent magnetic states are observed and isothermal measurements fail to probe the phase transition correctly. To explain the influence of the irreversible magnetostructural transition on the magnetic properties and magnetocaloric effects, we performed the $M(H)$ measurements with noncontinuous and continuous heating methods. The results of Figs. 3 and 4 confirm that the magnetostructural transitions are irreversible for the $Ni_{46.8}Cu_{2.5}Mn_{36.5}Sn_{14.3}$ and $Ni_{45.3}Cu_{4.5}Mn_{35.9}Sn_{14.3}$ alloys. On

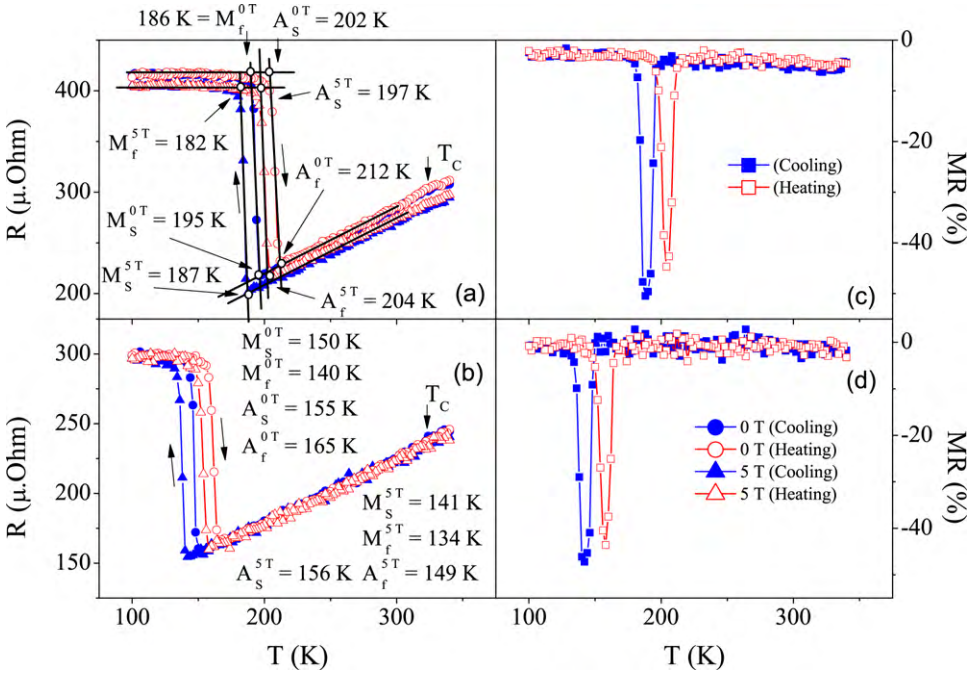

Fig. 5. The temperature dependence of the resistance of (a) $Ni_{46.8}Cu_{2.5}Mn_{36.5}Sn_{14.3}$ and (b) $Ni_{45.3}Cu_{4.5}Mn_{35.9}Sn_{14.3}$ at 0 and 5 T. The temperature dependence of the magnetoresistance for the both alloys (c) and (d).

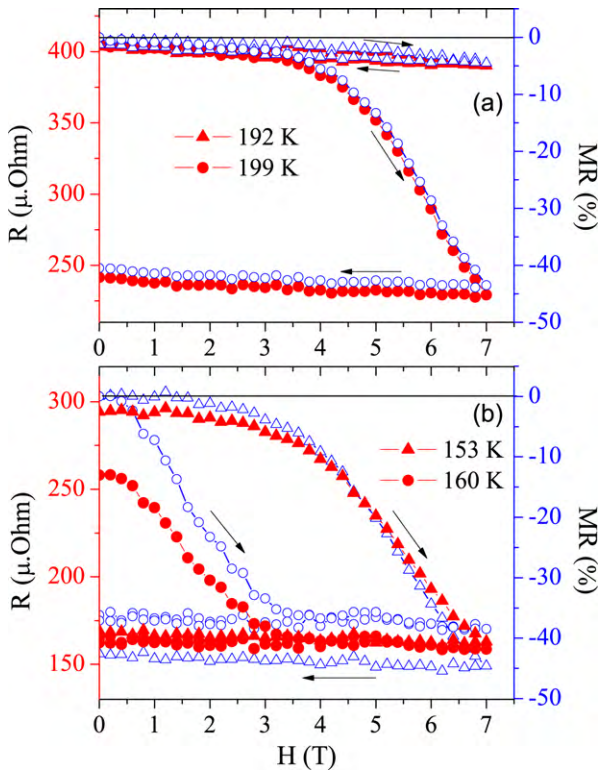

Fig. 6. Magnetic field dependence of the resistance (dark symbols) and magnetoresistance (open symbols) of (a) $Ni_{46.8}Cu_{2.5}Mn_{36.5}Sn_{14.3}$ and (b) $Ni_{45.3}Cu_{4.5}Mn_{35.9}Sn_{14.3}$ at different temperatures. The arrows show the direction of magnetic field changing.

the other hand, in magnetic refrigerations, the MCE materials are used in different thermodynamic cycles. When the MCE materials are moved under magnetic field in the magnetic refrigerators, the temperature of these materials decreases and increases. Therefore, we should use the $M(H)$ data which is measured in noncontinuous heating method to estimate ΔS_M using Maxwell equation since the noncontinuous method apply us the same conditions as magnetic refrigeration. In addition, since the magnetostructural transitions occur with large hysteresis, to observe the influence of the hysteresis on the estimating of MCE from $M(H)$ curves, we used the noncontinuous heating method.

Fig. 5(a) and (b) shows the temperature dependence of electrical resistance – $R(T)$ of the $Ni_{46.8}Cu_{2.5}Mn_{36.5}Sn_{14.3}$ and $Ni_{45.3}Cu_{4.5}Mn_{35.9}Sn_{14.3}$ alloys between 100 and 340 K, both in the heating and cooling cycles, under zero-field and 5 T. The austenite and martensite start and finish temperatures were also determined from the $R(T)$ curves as seen in Fig. 5. It is observed that the martensitic transition shifts towards lower temperature with increasing magnetic field. A very large $MR = \{[R(H) - R(0)]/R(0)\} \times 100]$ is observed in the martensitic transition region for both alloys (see Fig. 5(c) and (d)). For the magnetic field change of 5 T, the values of MR are about −46% and −43% for both alloys. The MR values of our alloys are higher than the value of the $Ni_{50}Mn_{34}Sn_{16}$ alloy (MR = −35%) for the same magnetic field change [19].

To investigate the type of magnetostructural transition, the magnetic field dependence of electrical resistance ($R(H)$) measurements was also performed for both alloys. Fig. 6(a) and (b) shows $R(H)$ and MR at the different temperatures for both alloys. For the $R(H)$ measurements, firstly the samples were cooled down to 100 K from 340 K and then the temperature went up to the desirable temperature to perform magnetic field dependence of resistance. We used the noncontinuous heating method for the measurement of the $R(H)$ curves to compare the resistance results with $M(H)$ curves. According to Fig. 6(a) and (b), increasing magnetic field causes the martensite to austenite transition and hence a sharp reduction in resistance is observed. But when the magnetic field decreases from 7 to 0 T, the sharp increasing in resistance is not observed. This means that when the magnetic field decreases from 7 to 0 T the reversible transition from austenite to martensite transition is not observed, the sample remains in the austenite phase. That is, the magnetostructural transition has magnetoplastic character (i.e. the magnetostructural transition is irreversible) for both alloys.

4. Conclusion

In conclusion, the decreasing of M_s temperatures is observed on this study with increasing the valence electron concentrations per atom e/a different from the results in the literature. According to our and earlier results, one can say that the e/a dependence of M_s temperature should be more complex in Ni-based Heusler alloys. The magnetic entropy change should be estimated using the $M(H)$ curves that are measured with noncontinuous heating method to recover the influence of irreversibility on magnetocaloric effect. The peak position and value of the magnetic entropy change are closely related to the sample history. The determination of the magnetic entropy change in alloys which show the irreversible magnetostructural transition has carefully been studied. The magnetic field dependence of resistance curves is in a good agreement with the noncontinuous $M(H)$ curves. The very large magnetoresistance associated with the martensitic transformation is observed in $(Ni–Cu)_{50}Mn_{36}Sn_{14}$ alloys.

Acknowledgments

This work was performed at the Magnetic Materials Research Laboratory in Ankara University and supported by Ankara University Research Funds (Grant Number: BAP 08B4343005)

References

[1] V.K. Pecharsky, K.A. Gschneidner Jr., A.O. Pecharsky, A.M. Tishin, Phys. Rev. B 64 (1998) 2045.
[2] M. Khan, A.K. Pathak, M.R. Paudel, I. Dubenko, S. Stadler, N. Ali, J. Magn. Magn. Mater. 320 (2008) L21.
[3] V.K. Sharma, M.K. Chattopadhyay, K.H.B. Shaeb, A. Chouhan, S.B. Roy, Appl. Phys. Lett. 89 (2006) 222509.
[4] A. Sozinov, A.A. Likhachev, N. Lanska, K. Ullakko, Appl. Phys. Lett. 80 (2002) 1746.
[5] Y. Suto, Y. Imano, N. Koeda, T. Omori, R. Kainuma, K. Ishida, K. Oikawa, Appl. Phys. Lett. 85 (2004) 4358.
[6] T. Krenke, E. Duman, M. Acet, E.F. Wassermann, X. Moya, L. Mañosa, A. Planes, E. Suard, B. Ouladdiaf, Phys. Rev. B 75 (2007) 104414.
[7] M. Pasquale, C.P. Sasso, L.H. Lewis, L. Giudici, T. Lograsso, D. Schagel, Phys. Rev. B 72 (2005) 094435.
[8] A. Kumar Pathak, M. Khan, I. Dubenko, S. Stadler, N. Ali, Appl. Phys. Lett. 90 (2007) 262504.
[9] T. Krenke, E. Duman, M. Acet, E.F. Wassermann, X. Moya, L. Mañosa, A. Planes, Nat. Mater. 4 (2005) 450.
[10] K. Koyama, H. Okada, K. Watanabe, T. Kanomata, R. Kainuma, W. Ito, K. Oikawa, K. Ishida, Appl. Phys. Lett. 89 (2006) 182510.
[11] Y.D. Wang, Y. Ren, E.W. Huang, Z.H. Nie, G. Wang, Y.D. Liu, J.N. Deng, L. Zuo, H. Choo, P.K. Liaw, D.E. Brown, Appl. Phys. Lett. 90 (2007) 101917.
[12] S. Chatterjee, S. Giri, S. Majumdar, S.K. De, Phys. Rev. B 77 (2008) 012404.
[13] L. Ma, H.W. Zhang, S.Y. Yu, Z.Y. Zhu, J.L. Chen, G.H. Wu, H.Y. Liu, J.P. Qu, Y.X. Li, Appl. Phys. Lett. 92 (2008) 032509.
[14] A. Planes, L. Mañosa, M. Acet, J. Phys.: Condens. Matter 21 (2009) 233201.
[15] K. Koyama, K. Watanabe, T. Kanomata, R. Kainuma, K. Oikawa, K. Ishida, Appl. Phys. Lett. 88 (2006) 132505.
[16] W. Ito, K. Ito, R.Y. Umetsu, R. Kainuma, K. Koyama, K. Watanabe, A. Fujita, K. Oikawa, K. Ishida, T. Kanomata, Appl. Phys. Lett. 92 (2008) 021908.
[17] T. Krenke, X. Moya, S. Aksoy, M. Acet, P. Entel, L. Mañosa, A. Planes, Y. Elerman, A. Yücel, E.F. Wassermann, J. Magn. Magn. Mater. 310 (2007) 2788.
[18] L. Caron, Z.Q. Ou, T.T. Nguyen, D.T. Cam Thanh, O. Tegus, E. Brück, J. Magn. Magn. Mater. 321 (2009) 3559.
[19] S. Chatterjee, S. Giri, S. Majumdar, S.K. De, J. Phys. D: Appl. Phys. 42 (2009) 065001.